ChemComm

COMMUNICATION

View Article Online
View Journal | View Issue

Cite this: *Chem. Commun.*, 2014, **50**, 11204

Received 18th June 2014,
Accepted 5th August 2014

DOI: 10.1039/c4cc04642k

www.rsc.org/chemcomm

Local protonation control using plasmonic activation†

Pushkar Singh[a] and Volker Deckert*[ab]

Localized protonation of 4-mercaptopyridine (4-MPY), activated by light in the presence of silver nanoparticles is monitored under ambient conditions using surface-enhanced Raman scattering (SERS) and tip-enhanced Raman scattering (TERS). The reaction can be controlled by the excitation wavelength and the atmospheric conditions, thus, providing a tool for site-specific control of protonation.

Coupling of electromagnetic radiation under specific conditions to a metal–dielectric interface results in surface plasmons (SP), which play a key role in many areas like biosensors,[1,2] DNA sequencing,[3,4] plasmon microscope,[5–7] dissociation of H_2,[8] splitting of water[9–11] *etc.* Controlling chemical reactions by light-induced catalytic processes is a long-standing goal in physical chemistry. Recently, surface plasmon induced chemical reactions are gaining much attention. For instance, reduction reaction,[12,13] oxidation reaction[14,15] and pH dependence[16,17] have been reported. In this communication we will focus on the reaction of an immobilized pyridine compound as an example for a plasmon assisted protonation.

To our knowledge, this is the first experimental report discussing a protonation reaction induced by surface plasmons under ambient conditions (Scheme 1). The experiments were performed under ambient conditions and we hypothesize that the proton generation is based on the dissociation of atmospheric water. Dissociation of atmospheric hydrogen seems unlikely, however, cannot be entirely excluded at present. The hypothesis is confirmed by SERS experiments under inert atmosphere (argon) where no protonation signature was observed.

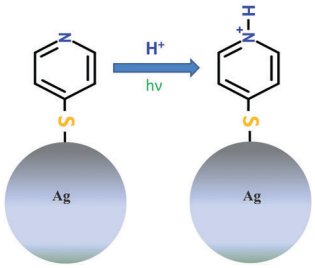

Scheme 1 Protonation of 4-MPY in the presence of metal nanoparticles and light.

In the present study 4-mercaptopyridine (4-MPY) was chosen as a model compound for plasmon induced protonation. The adsorption of 4-MPY on metal surfaces can occur *via* three potential sites (1) the sulphur function, (2) *via* lone pair electrons of the nitrogen and (3) *via* aromatic π-electrons of the ring. Previous studies on different metal surfaces (Ag, Au and Pt) strongly suggest the binding of 4-MPY through the S atom by cleavage of the S–H bond.[18–21] Furthermore, pH dependent surface enhanced Raman scattering (SERS) studies of 4-MPY show that at pH > 12 the unprotonated (UP) compound is observed. This is indicated by a single Raman peak at 1575 cm^{-1} (ring stretching mode with unprotonated nitrogen). Decreasing the pH < 1 results in a loss of this peak while, at 1608 cm^{-1} a new signal appears, that is assigned to ring stretching mode with a protonated nitrogen (PN).[18,20,22–24] Protonation on SERS substrates has been studied on various molecular systems[22,25–27] using different experimental techniques and all these studies show a pH dependency. Generally, the protonation is reversible and depending on the pH conditions, protonation and deprotonation can be observed.

For the detailed investigation of such surface dependent reactions, a site specific detection at single molecule level would be extremely valuable. Tip-enhanced Raman scattering (TERS) provides a tool to investigate structural information of surfaces with nanometre resolution using a plasmonic hot spot at a scanning probe tip to probe the sample interface. The electromagnetic field

[a] *Leibniz Institute of Photonic Technology, Albert-Einstein-Str. 9, 07745 Jena, Germany*
[b] *Institute of Physical Chemistry and Abbe Center of Photonics, Friedrich-Schiller University Jena, Helmholtzweg 4, 07743 Jena, Germany. E-mail: volker.deckert@ipht-jena.de*

† Electronic supplementary information (ESI) available: Experimental details, preparation of SERS substrate, synthesis of gold nanoplates. See DOI: 10.1039/c4cc04642k

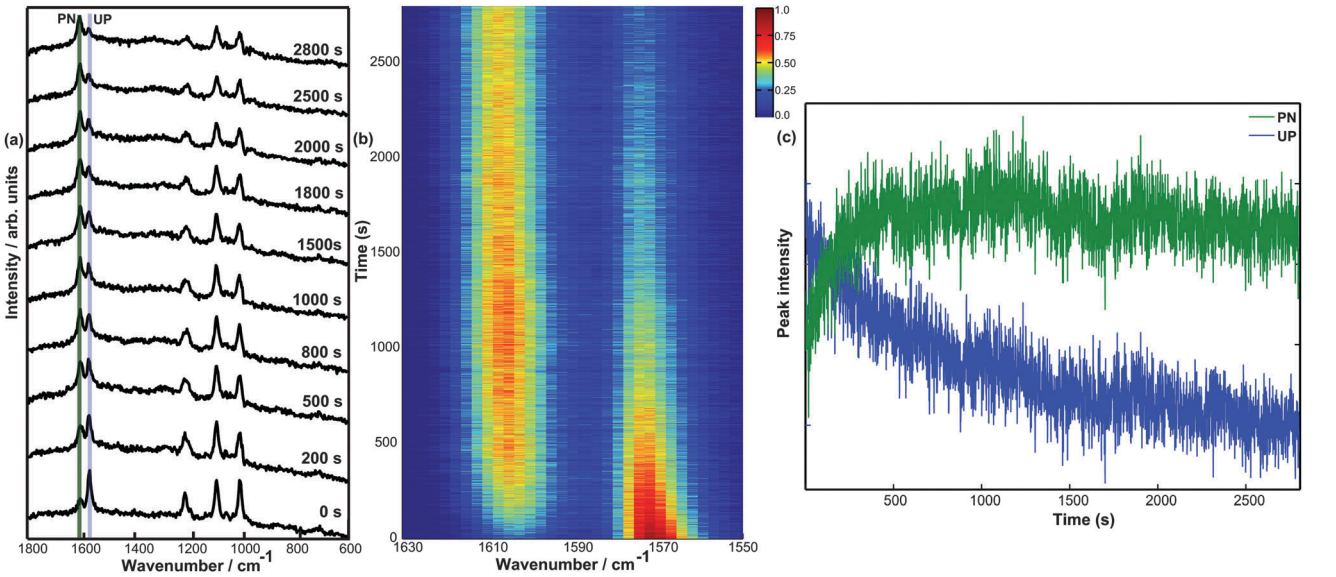

Fig. 1 (a) Selected time-dependent SERS spectra of 4-MPY under 532 nm/125 μW laser radiation, acquisition time of 1 s. (b) SERS intensity plot of the full series in a wavenumbers range from 1550–1630 cm^{-1}. (c) Integrated peak intensity of the protonated peak in green and unprotonated peak in blue. The bands are assigned as 1006 cm^{-1} (ring breathing), 1092 cm^{-1} (ring breathing/C–S), 1211 cm^{-1} (β(CH)/δ(NH)), 1575 cm^{-1} (ring stretching mode with unprotonated nitrogen (UP)) and 1608 cm^{-1} (ring stretching mode with protonated nitrogen (PN)).

enhancement at this hot spot leads to a Raman signal enhancement of several orders of magnitude and even single molecule sensitivity has been demonstrated.[28–32] Recently it has been shown that surface plasmon induced chemical reactions can be monitored using TERS under ambient conditions and also under ultrahigh vacuum conditions.[12,13] In the present study we use a combined SERS and TERS approach to investigate the protonation of 4-MPY.

Initially SERS spectra of 4-MPY adsorbed on silver island films using a laser wavelength of 532 nm at 125 μW were measured over several minutes. Fig. 1a shows 10 selected spectra measured at different time-points. Initially Raman band at 1575 cm^{-1} (indicating the unprotonated compound) with high intensity and a very small protonated band at 1608 cm^{-1} is visible. Gradually the Raman band at 1608 cm^{-1} increases indicating the protonation of 4-MPY. Thus a conversion from unprotonated to protonated 4-MPY is monitored. Fig. 1b clarifies this conversion in the form of a colour coded intensity plot. The results suggest that a proton source must be present, as no further reaction of the 4-MPY (*e.g.* decomposition) could be detected. Different hydrogen containing components in air could be responsible for the observations. As the dissociation of H_2[8] and H_2O[9–11] under surface plasmon conditions were already shown, this further strengthens our assumption of protonation of 4-MPY using surface plasmon under ambient conditions. Fig. 1c shows the intensity of unprotonated and protonated peak as time progresses. One can see that the intensity of the protonated peak increases initially and reaches to a maximum. We also noticed that the intensity of different peaks shown in Fig. 1a decrease as time progresses. This could be attributed to an oxidation of the silver island film during the measurement. This effect will not be discussed further as it will not affect the main conclusion of this work.

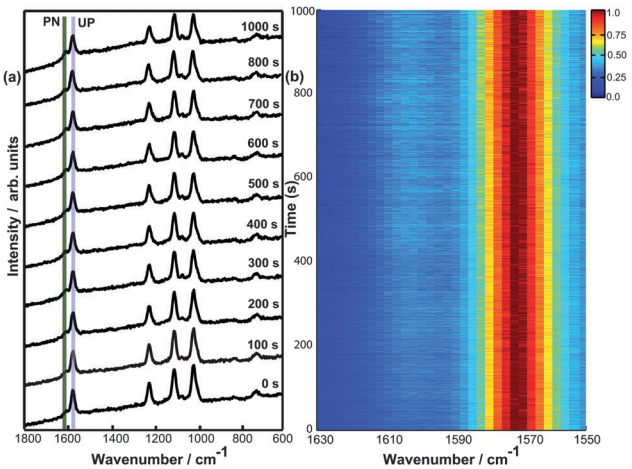

Fig. 2 (a) Time-dependent SERS spectra of 4-MPY under a continuous flow of argon during the experiment. Laser excitation at 532 nm/150 μW, integration time 1 s. (b) Colour coded intensity plot of same series in wavenumbers range from 1550–1630 cm^{-1}. No protonation is observed.

Considering H_2O or H_2 under ambient as a possible hydrogen sources required for the surface plasmon induced protonation reaction, we performed time dependent measurements under a continuous flow of argon. Fig. 2a shows the time development of 10 spectra at different times-points. The data clearly indicate that no protonation takes place. Fig. 2b shows all time dependent SERS spectra as a colour coded intensity plot.

It has been shown experimentally and theoretically that silver nanoparticles generate higher electromagnetic field enhancement under 532 nm radiation compared to 632 nm as the resonance wavelength of the silver nanoparticles (diameter 100 nm) used in the present study is very close to 532 nm.[33–35] Consequently, employing

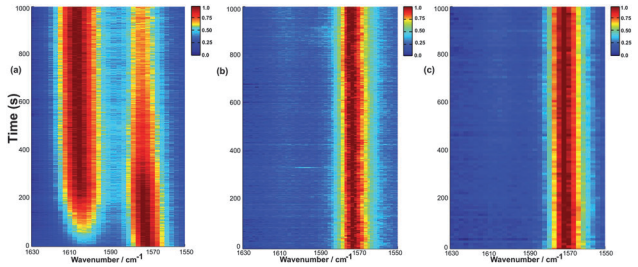

Fig. 3 (a) Colour coded SERS intensity plot of 4-MPY under 532 nm laser radiation with laser power of 50 μW with an integration time of 2 s, clearly show protonation as a function of time. (b) SERS intensity plot of 4-MPY under 632 nm/50 μW laser radiation, integration time 4 s; no protonation is observed (c) SERS intensity plot of 4-MPY under 532 nm/18 μW laser radiation, integration time of 10 s; under low power conditions no protonation is observed either.

the same incident laser power (50 μW) and 632 nm laser excitation (Fig. 3b) compared to 532 nm (Fig. 3a), no protonation could be detected, thus the intensity of the surface plasmon with 632 nm excitation is not sufficient to start the reaction. Low power (18 μW) of 532 nm laser excitation (see Fig. 3c) shows also no protonation signature. Thus a minimum intensity of surface plasmon is the decisive factor to initiate the protonation which can be controlled using either incident laser power or excitation wavelength.

The results of different excitation wavelengths at 50 μW further imply that the protonation reaction is not induced due to a temperature increase in the laser focus since under same laser power the temperature should be approximately the same. To further investigate the temperature dependence we performed temperature dependent experiments. A low incident power (12 μW @ 532 nm) was used such that no protonation could be observed at room temperature, increasing the temperature of the substrate up to 60 °C (data not shown), did not yield the protonation either.

In comparison to SERS where many nanoparticles are present in the laser focus and contribute to the overall Raman signal, in tip-enhanced Raman scattering (TERS) the signal is generated from a silver coated AFM tip of about 10 nm in radius and thus reducing the enhancing unit to a single nanoparticle. In a TERS experiment the silver coated AFM tip is positioned in the laser focus, thus only one specific plasmonic feature contributes to the signal. In order to warrant similar conditions a monolayer of 4-MPY was immobilized on a flat transparent gold nanoplate[36,37] (see ESI† for detail).

Fig. 4a shows 10 selected TERS spectra under ambient conditions and Fig. 4b shows the time-dependent TERS spectra plotted as a colour coded intensity plot. Interestingly under TERS conditions a much faster protonation of 4-MPY was observed compared to SERS. A control TERS measurement was also performed under inert atmosphere. Fig. 4c shows 10 selected spectra of TERS measurement under inert atmosphere at different time-points and Fig. 4d shows the corresponding time dependent TERS spectra plotted as a colour coded intensity plot. The results nicely confirm the role of atmospheric conditions as seen in the SERS experiments. The difference between Au and Ag as the binding site has surprisingly little effect to the band positions of the protonated and unprotonated peaks.

With respect to the "instantaneous" protonation, previous theoretical and experimental studies showed that field confinement between two metal nanoparticles leads to an increased enhancement.[38,39] This effect also occurs in a particle-on-metal-surface geometry ("gap-mode") as in the case of the TERS experiment. Furthermore the tip-sample nanogap allows an efficient electron transfer from tip to sample.[40,41] These effects can explain a faster protonation under TERS conditions with very defined and optimized geometry, whereas under SERS conditions many sites with different efficiencies contribute to the overall signal changes. Hence, in the case of the SERS experiments a gradual protonation is observed. To exclude any power related aspects a SERS experiment also using 650 μW (data not shown) was done and a comparable behavior regarding an increase in the reaction rate was observed which also

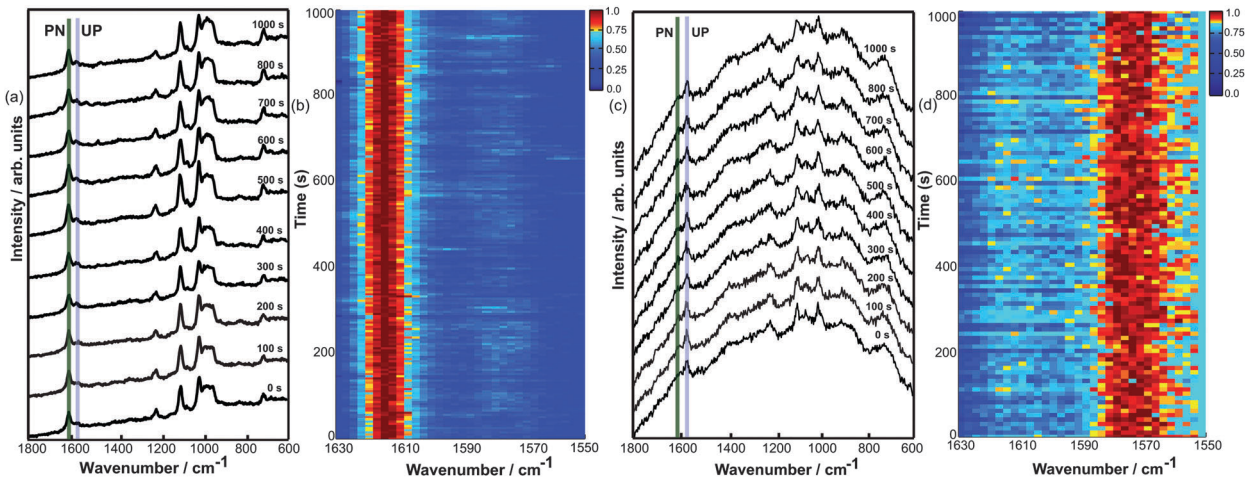

Fig. 4 (a) Time-dependent TERS spectra of 4-MPY under ambient conditions (excitation 532 nm/650 μW; integration time 5 s), (b) colour coded intensity plot of the data (a) wavenumbers range from 1550–1630 cm^{-1}, (c) time-dependent TERS spectra of 4-MPY under argon (excitation 532 nm/650 μW; integration time 10 s). (d) TERS intensity plot of the data in (c) wavenumbers range from 1550–1630 cm^{-1}.

agrees with recent power dependent SERS measurement on 4-MPY.[24] We also like to note a difference in the appearance of a broad peak around 980 cm^{-1} in TERS measurements. This peak is due to silicon tip and its nature changes from tip to tip. Since the TERS experiments with and without argon were performed with different tips, a direct comparison regarding the spectral background is difficult.

In conclusion, we report the experimental observation of protonation reaction under ambient condition using 4-MPY as a model system. While the actual mechanism of the protonation cannot be revealed with the presented experiments, it demonstrates the conditions under which the surface catalytic reaction can be controlled. The control experiment under a continuous flow of argon confirms that atmospheric H_2O (H_2 cannot be fully excluded yet) acts as a potential proton source required for the reaction. The study further demonstrates that the intensity of the surface plasmon is a key factor to initiate the protonation reaction. The TERS experiments not only confirm the findings of the SERS, but also demonstrate a site specific protonation catalyst that can be located at specific sites and synchronously act as a structurally specific sensor. Interestingly, despite the lower number of plasmonic particles in the case of TERS the protonation happen much faster compared to SERS. This can be attributed to large electromagnetic fields produced in the metal–metal nanogap between tip and substrate and an efficient electron transfer. Consequently, the observed reaction depends more on the specific nanoparticle activity rather than the number of particles. This opens interesting perspective for site specific protonation with nanometre control.

Financial Support from the European Union and the state of Thuringia (FKZ: 2011 FE 9048; 2011 VF 0016) as well as through the Deutsche Forschungsgemeinschaft (FR 1348/19-1) is gratefully acknowledged.

Notes and references

1 M. Piliarik, H. Šípová, P. Kvasnička, N. Galler, J. R. Krenn and J. Homola, *Opt. Express*, 2012, **20**, 672–680.
2 J. Zhao, X. Zhang, C. R. Yonzon, A. J. Haes and R. P. Van Duyne, *Nanomedicine*, 2006, **1**, 219–228.
3 K. Nakatani, S. Sando and I. Saito, *Nat. Biotechnol.*, 2001, **19**, 51–55.
4 R. Robelek, L. Niu, E. L. Schmid and W. Knoll, *Anal. Chem.*, 2004, **76**, 6160–6165.
5 B. Rothenhäusler and W. Knoll, *Nature*, 1988, **332**, 615–617.
6 M. G. Somekh, S. Liu, T. S. Velinov and C. W. See, *Appl. Opt.*, 2000, **39**, 6279–6287.
7 B. Gjonaj, J. Aulbach, P. M. Johnson, A. P. Mosk, L. Kuipers and A. Lagendijk, *Phys. Rev. Lett.*, 2013, **110**, 266804.
8 S. Mukherjee, F. Libisch, N. Large, O. Neumann, L. V. Brown, J. Cheng, J. B. Lassiter, E. A. Carter, P. Nordlander and N. J. Halas, *Nano Lett.*, 2013, **13**, 240–247.
9 D. B. Ingram and S. Linic, *J. Am. Chem. Soc.*, 2011, **133**, 5202–5205.
10 J. Lee, S. Mubeen, X. Ji, G. D. Stucky and M. Moskovits, *Nano Lett.*, 2012, **12**, 5014–5019.
11 C. G. Silva, R. Juárez, T. Marino, R. Molinari and H. García, *J. Am. Chem. Soc.*, 2011, **133**, 595–602.
12 E. M. v. Schrojenstein Lantman, T. Deckert-Gaudig, A. J. G. Mank, V. Deckert and B. M. Weckhuysen, *Nat. Nanotechnol.*, 2012, **7**, 583–586.
13 M. Sun, Z. Zhang, H. Zheng and H. Xu, *Sci. Rep.*, 2012, **2**, 647.
14 P. Christopher, H. Xin and S. Linic, *Nat. Chem.*, 2011, **3**, 467–472.
15 W. H. Hung, M. Aykol, D. Valley, W. Hou and S. B. Cronin, *Nano Lett.*, 2010, **10**, 1314–1318.
16 Y. Toh, P. Yu, X. Wen, J. Tang and T. Hsieh, *Nanoscale Res. Lett.*, 2013, **8**, 103.
17 M. Sun, Z. Zhang, Z. H. Kim, H. Zheng and H. Xu, *Chem. – Eur. J.*, 2013, **19**, 14958–14962.
18 J. Baldwin, N. Schühler, I. S. Butler and M. P. Andrews, *Langmuir*, 1996, **12**, 6389–6398.
19 M. A. Bryant, S. L. Joa and J. E. Pemberton, *Langmuir*, 1992, **8**, 753–756.
20 H. S. Jung, K. Kim and M. S. Kim, *J. Mol. Struct.*, 1997, **407**, 139–147.
21 T. Sueoka, J. Inukai and M. Ito, *J. Electron Spectrosc. Relat. Phenom.*, 1993, **64–65**, 363–370.
22 J. Hu, B. Zhao, W. Xu, B. Li and Y. Fan, *Spectrochim. Acta, Part A*, 2002, **58**, 2827–2834.
23 J. A. Baldwin, B. Vlčková, M. P. Andrews and I. S. Butler, *Langmuir*, 1997, **13**, 3744–3751.
24 X. S. Zheng, P. Hu, J. H. Zhong, C. Zong, X. Wang, B. J. Liu and B. Ren, *J. Phys. Chem. C*, 2014, **118**, 3750–3757.
25 J. Herranz, F. Jaouen, M. Lefevre, U. I. Kramm, E. Proietti, J. Dodelet, P. Bogdanoff, S. Fiechter, I. Abs-Wurmbach, P. Bertrand, T. M. Arruda and S. Mukerjee, *J. Phys. Chem. C*, 2011, **115**, 16087–16097.
26 H. T. Miles, F. B. Howard and J. Frazier, *Science*, 1963, **142**, 1458–1463.
27 D. B. Spry and M. D. Fayer, *J. Phys. Chem. B*, 2009, **113**, 10210–10221.
28 C. C. Neacsu, J. Dreyer, N. Behr and M. B. Raschke, *Phys. Rev. B: Condens. Matter Mater. Phys.*, 2006, **73**, 193406.
29 M. D. Sonntag, J. M. Klingsporn, L. K. Garibay, J. M. Roberts, J. A. Dieringer, T. Seideman, K. A. Scheidt, L. Jensen, G. C. Schatz and R. P. Van Duyne, *J. Phys. Chem. C*, 2012, **116**, 478–483.
30 R. Zhang, Y. Zhang, Z. C. Dong, S. Jiang, C. Zhang, L. G. Chen, L. Zhang, Y. Liao, J. Aizpurua, Y. Luo, J. L. Yang and J. G. Hou, *Nature*, 2013, **498**, 82–86.
31 E. Bailo and V. Deckert, *Angew. Chem., Int. Ed.*, 2008, **47**, 1658–1661.
32 T. Deckert-Gaudig, R. Böhme, E. Freier, A. Sebesta, T. Merkendorf, J. Popp, K. Gerwert and V. Deckert, *J. Biophotonics*, 2012, **5**, 582–591.
33 B. Dong, Y. Fang, X. Chen, H. Xu and M. Sun, *Langmuir*, 2011, **27**, 10677–10682.
34 L. Kang, P. Xu, B. Zhang, H. Tsai, X. Han and H. L. Wang, *Chem. Commun.*, 2013, **49**, 3389–3391.
35 R. Stöckle, V. Deckert, C. Fokas and R. Zenobi, *Appl. Spectrosc.*, 2000, **54**, 1577–1583.
36 T. Deckert-Gaudig, E. Bailoa and V. Deckert, *Phys. Chem. Chem. Phys.*, 2009, **11**, 7360–7362.
37 T. Deckert-Gaudig and V. Deckert, *Small*, 2009, **5**, 432–436.
38 M. Futamata, Y. Maruyama and M. Ishikawa, *J. Phys. Chem. B*, 2003, **107**, 7607–7617.
39 T. Yanoa, T. Ichimuraa, A. Taguchi, N. Hayazawaa, P. Vermaa, Y. Inouyea and S. Kawataa, *Appl. Phys. Lett.*, 2007, **91**, 121101.
40 K. J. Savage, M. M. Hawkeye, R. Esteban, A. G. Andrei, G. Borisov, J. Aizpurua and J. J. Baumberg, *Nature*, 2012, **491**, 574–577.
41 Z. Zhang, M. Sun, P. Ruan, H. Zheng and H. Xu, *Nanoscale*, 2013, **5**, 4151–4155.